

Pilot Equalization in Manual Control of Aircraft Dynamics

D.M. Pool, P.M.T. Zaal, H.J. Damveld, M.M. van Paassen and M. Mulder
Control and Simulation Division

Faculty of Aerospace Engineering, Delft University of Technology
Delft, The Netherlands

d.m.pool@tudelft.nl, p.m.t.zaal@tudelft.nl, h.j.damveld@tudelft.nl, m.m.vanpaassen@tudelft.nl and m.mulder@tudelft.nl

Abstract—In continuous manual control tasks, pilots adapt their control strategy to the dynamics of the controlled element to yield adequate performance of the combined pilot-vehicle system. For a controlled element representing the linearized pitch dynamics of a small jet aircraft, the pilot models described in literature were found to lack the required freedom in the pilot equalization term to accurately model the adopted pilot compensation. An additional lead term in the pilot equalization transfer function was found to significantly increase the accuracy in modeling manual control behavior of aircraft pitch dynamics.

Index Terms—Manual control, pilot modeling, identification

I. INTRODUCTION

Recently, a renewed interest has arisen in modeling pilot control behavior in manual aircraft control tasks, for instance in assessment of flight simulator fidelity [1]–[3] and the evaluation of aircraft handling qualities [4], [5]. These research efforts attempt to use measured changes in pilot control behavior in manual tracking tasks, often visualized through the use of pilot models, to indicate degraded simulator fidelity or handling qualities.

Many studies into the dynamics of human pilots in tracking tasks are described in literature. The foundations have been laid by Elkind [6] and McRuer et al. [7], [8] for single-loop compensatory manual target tracking tasks with a visually presented, random-appearing forcing function. Based on their Crossover Model theorem, McRuer et al. introduced a quasi-linear model for describing human operation and adaptation during compensatory tracking [7]. The model comprises two elements: a generalized pilot describing function form and a set of rules for adjusting the model to control-task specific characteristics such as controlled element dynamics and forcing function bandwidth. In slightly simplified form compared to [7], the generalized pilot describing function is given by:

$$H_p(j\omega) = K_p \underbrace{\left(\frac{T_L j\omega + 1}{T_I j\omega + 1} \right)}_{\text{pilot equalization}} e^{-j\omega\tau} H_{nm}(j\omega) \quad (1)$$

The pilot model defined by (1) accounts for pilot time delay (τ) and the characteristics of the human neuromuscular system through $H_{nm}(j\omega)$. The remainder of (1) represents the pilot equalization characteristic and is the main means for describing pilot adaptation.

In general, the pilot model adjustments can be divided into two categories: adaptation and optimization. Broadly speaking, adaptation involves the operator's selection of a specific equalization form. In manual control tasks, human operators are seen to adapt their control behavior to yield a pilot-vehicle system that has the properties of a well-designed feedback control system, that is, approximately have single integrator dynamics over a significant frequency range around the gain crossover frequency [8]. Depending on the dynamics of the controlled element, the full lead-lag equalization shown in (1) may therefore be reduced to a pure lead, pure lag or pure gain. After an appropriate equalization is selected, the parameters of the selected model structure are set to satisfy some internally generated criteria in the optimization step of the model adjustment.

It is generally accepted that the pilot equalization consists of at most one lead term and one lag term as defined in (1). McRuer et al. [7], [8] have demonstrated that (1) can model pilot control behavior for pure gain, single and double integrator dynamics, as well as for conditionally stable first and second-order systems. In addition, in [9] it is explicitly suggested that for aircraft applications an appropriate pilot equalization would be comprised of one lead and one lag term.

Later studies performed by Steurs et al. [1], Groot et al. [4], Zaal et al. [2] and Damveld [5], however, indicated that a lead-lag equalization as defined in (1) does not always suffice for modeling manual control of conventional aircraft pitch dynamics. Therefore, the main objective of the present study is to obtain the appropriate pilot model structure and parameters of the pilot equalization in the manual control of aircraft pitch dynamics during a compensatory tracking task. Additionally, the influence of supplying physical motion cues in the controlled degree of freedom on the adopted pilot equalization is investigated.

The objective will be achieved by measuring pilot control behavior in a compensatory tracking task – controlling a linearized reduced-order model of the pitch dynamics of a Cessna Citation I business jet – in the SIMONA Research Simulator (SRS). In order to investigate the influence of motion feedback, the task will be performed both with and without motion cues. To be able to investigate the separate contributions of the visual and vestibular systems, a combined disturbance-rejection and target-following task is performed [2], [3], [10].

To confirm that the requirement for a more complex model for pilot equalization is indeed caused by the aircraft dynamics, the experiment has been repeated for control of a system with double integrator dynamics, both with and without motion.

II. PILOT COMPENSATION IN MANUAL CONTROL

A. Control Task

Fig. 1 shows a schematic representation of the compensatory control task that is considered in the present study. The pilot is presented an error signal e on a visual display, resulting from the target and disturbance forcing function signals, f_t and f_d . If the motion of the controlled element H_{θ,δ_e} is presented through physical motion cues in addition to the visually perceived error, an additional feedback path is present that provides the pilot with state information. Fig. 1 differs from the tasks considered by McRuer et al. [7] by the presence of the motion feedback path $H_{p_m}(j\omega)$ and the disturbance f_d . If no motion feedback is available, however, the disturbance signal and the target signal are equivalent due to the compensatory display, and the task becomes exactly equal to the single-loop tasks studied by McRuer et al.

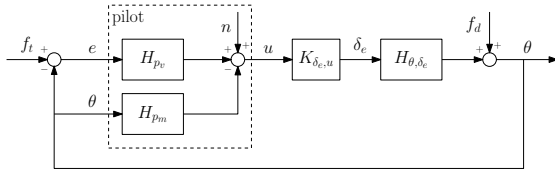


Fig. 1. Compensatory pitch attitude control task.

B. Multimodal Pilot Model

Many different model structures have been derived in past studies to represent the pilot's response to visual errors $H_{p_v}(j\omega)$ and perceived pitch accelerations $H_{p_m}(j\omega)$, such as the Descriptive Model [11], the Crossover Model, the Extended Crossover Model and the Precision Model [7]. The present study adopted a combination of the Precision Model for the visual response, and the Descriptive Model for the vestibular pitch acceleration response. The model is shown in Fig. 2.

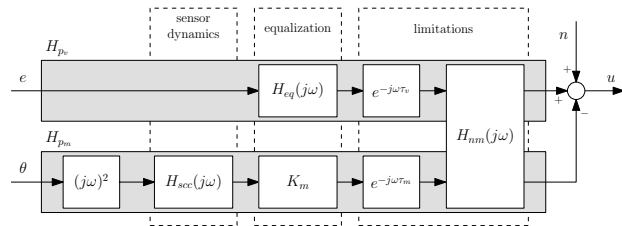


Fig. 2. Multimodal pilot model.

Note that the visual channel of the pilot model depicted in Fig. 2 is largely equivalent to (1), where the lead-lag equalization has been replaced by the transfer function $H_{eq}(j\omega)$. The additional motion channel of the pilot model incorporates the

pilot's response to his vestibular motion sensation. The dynamics of the semicircular canals, the vestibular sensors that are sensitive to angular motion, are defined by $H_{sec}(j\omega)$, whose characteristic is taken from literature [11]. The neuromuscular system $H_{nm}(j\omega)$ is modeled as a second-order mass-spring-damper system with two parameters: the eigenfrequency ω_{nm} and damping ζ_{nm} . The main subject of investigation in this paper is the visual equalization term $H_{eq}(j\omega)$, as its structure is found to rely heavily on the dynamics of the system that is controlled.

C. Controlled Dynamics

In this paper, data from two sets of experiments are compared. Both experiments investigated the effect of motion feedback in a pitch attitude tracking task as depicted by Fig. 1. The first experiment evaluated the effects of pitch and heave motion cues on pilot control behavior in a pitch control task [2]. The controlled dynamics, H_{θ,δ_e} , in this experiment were the reduced-order linearized pitch dynamics of a Cessna Citation I Ce 500 business jet aircraft, in cruise at an altitude of 10,000 ft at an airspeed of 160 kts, as given by:

$$H_{\theta,\delta_e}(s) = 10.6189 \frac{s + 0.9906}{s(s^2 + 2.756s + 7.612)} \quad (2)$$

The Bode frequency response of the Citation pitch dynamics is depicted in Fig. 3. The second-order term in the denominator of (2) represents the short period mode, which for this aircraft is characterized by a natural frequency ω_{sp} and damping ζ_{sp} of 2.76 rad/s and 0.50, respectively. Note the significant magnitude peak and phase lead around the short period frequency. Furthermore, observe that the short period frequency is in the frequency range where the pilot-vehicle system crossover frequency is expected to be, that is 2-5 rad/s [8].

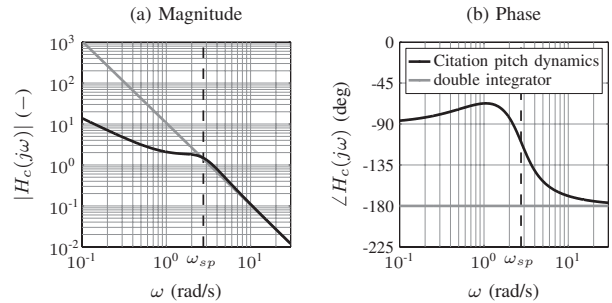


Fig. 3. Controlled dynamics frequency responses.

Previous experiments that investigated manual control behavior of aircraft pitch dynamics [1], [2], [4], [5] indicated that pilot equalization as defined in (1) is not sufficient for describing control behavior. To allow for comparison of these findings the results described by McRuer et al. [7], the same pitch tracking task described in [2] was performed in a later experiment with double integrator dynamics:

$$H_{\theta,\delta_e}(s) = 10.6189 \frac{1}{s^2}, \quad (3)$$

whose frequency response is depicted in Fig. 3 in gray.

D. Pilot Equalization

The theory of manual vehicle control as compiled by McRuer et al. [7]–[9] states pilots adapt their equalization strategy to the controlled element dynamics to yield a pilot-vehicle system that has the properties close to those of a single integrator system around the crossover frequency. For double integrator systems as defined by (3), it has been shown in literature

that pilot equalization takes the form of a pure lead in order to achieve these open-loop characteristics [11].

As indicated in Fig. 4, to achieve a pilot-vehicle system with approximate single integrator characteristics for control of (2), pilot equalization would need to be a gain at low frequencies, while high-frequency lead is required to compensate for the second-order dynamics at high frequencies. For the gain-like response of (2) below the short-period frequency, however, pilot lag would be required. Note that pilot equalization dynamics that achieve both pilot lag at low frequencies and lead at high frequencies can not be described with (1), as a second lead term is required to model this transition. Therefore, four different equalization models, which are listed in Tab. I, are evaluated for describing pilot control behavior in a pitch attitude tracking task in this study.

TABLE I
DEFINITION OF DIFFERENT EQUALIZATION SETTINGS.

Symb.	Equalization structure, $H_{eq}(j\omega)$
A	$K_v(1 + T_L j\omega)$
B	$K_v \frac{(1 + T_L j\omega)}{(1 + T_I j\omega)}$
C	$K_v \frac{(1 + T_L j\omega)^2}{(1 + T_I j\omega)}$
D	$K_v \frac{(1 + T_{L1} j\omega)(1 + T_{L2} j\omega)}{(1 + T_I j\omega)}$

Equalizations A and B represent pure lead and lead-lag equalization terms that have been frequently applied in literature. Equalizations C and D both have an additional lead term, to allow for modeling of pilot equalization of the form depicted in Fig. 4. The difference between both is that D allows for the additional lead time constant, T_{L2} , to have a different value than the first and thereby adds an extra parameter to the pilot model, while C assumes both lead time constants to be equal.

Pilot lead equalization captures pilots' perception of visual rate [11]. Note, however, that the additional lead term in the pilot model equalization for C and D does not imply modeling of pilot visual acceleration perception. Fig. 4 clearly illustrates that due to the fact that pilot lag is generated at

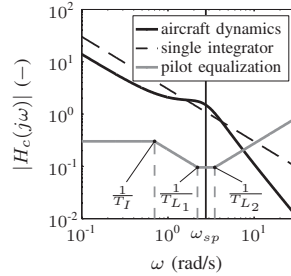


Fig. 4. Controlled aircraft dynamics frequency response magnitude and theoretical pilot equalization.

lower frequencies than pilot lead ($T_I > T_{L1,2}$), the effective pilot equalization will never be more than a single lead.

III. EXPERIMENT

A. Forcing Functions

The pitch tracking task considered in the experiments described in this paper (see Fig. 1) was defined to be a disturbance-rejection task, where the disturbance of the pitch attitude was induced by the disturbance signal f_d . An additional target signal f_t of small magnitude was inserted as well, this to facilitate multimodal pilot model identification [3], [10]. As in the experiments described by McRuer et al. [7], the forcing function signals were constructed as sums of ten sinusoids:

$$f_{d,t}(t) = \sum_{k=1}^{N_{d,t}} A_{d,t}(k) \sin(\omega_{d,t}(k)t + \phi_{d,t}(k)) \quad (4)$$

The forcing function frequency, amplitude and phase distributions ($\omega_{d,t}(k)$, $A_{d,t}(k)$ and $\phi_{d,t}(k)$) were the same as those used in a previous experiment [2]. The frequencies, amplitudes and phases of the target and disturbance signals are summarized in Tab. II.

TABLE II
EXPERIMENT FORCING FUNCTION PROPERTIES.

k (-)	disturbance, f_d				target, f_t			
	n_d (-)	ω_d (rad/s)	A_d (deg)	ϕ_d (rad)	n_t (-)	ω_t (rad/s)	A_t (deg)	ϕ_t (rad)
1	5	0.383	1.343	1.530	6	0.460	0.698	1.288
2	11	0.844	1.016	5.967	13	0.997	0.488	6.089
3	23	1.764	0.506	1.000	27	2.071	0.220	5.507
4	37	2.838	0.258	6.117	41	3.145	0.119	1.734
5	51	3.912	0.157	6.145	53	4.065	0.080	2.019
6	71	5.446	0.095	2.692	73	5.599	0.049	0.441
7	101	7.747	0.060	1.895	103	7.900	0.031	5.175
8	137	10.508	0.043	3.153	139	10.661	0.023	3.415
9	171	13.116	0.036	3.570	194	14.880	0.018	1.066
10	226	17.334	0.030	3.590	229	17.564	0.016	3.479

B. Apparatus

The experiments were performed in the SRS at Delft University of Technology, see Fig. 5. The SRS motion system was used to present the subjects with rotational pitch motion cues during specific conditions of both experiments. No motion filter (washout) was used for generating the pitch motion. The time delay associated with the SRS motion base is 30 ms.

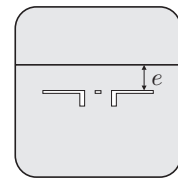
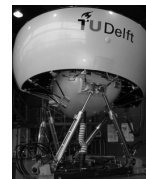


Fig. 5. The SIMONA Research Simulator. Fig. 6. Compensatory display.

The pitch tracking error the participants were to minimize during the tracking tasks was presented on a compensatory

visual display in the SRS cockpit. As indicated in Fig. 6, the pitch attitude of a simplified artificial horizon image indicated the instantaneous value of the tracking error e . The time delay associated with the generation of visual images on the SRS cockpit displays has been determined to be 20-25 ms.

In both experiments, subjects controlled the pitch dynamics with an electrical sidestick without break-out force and a maximum deflection of 14 deg. A gain factor controlled the scaling between sidestick deflections u to elevator inputs to the controlled dynamics δ_e . To give optimal control authority for both types of controlled dynamics, this gain – indicated with the symbol $K_{\delta_e, u}$ in Fig. 1 – was set to -0.2865 or -0.4011 for Citation or double integrator controlled elements, respectively.

C. Conditions, Participants and Experimental Procedure

Data from four different experimental conditions are evaluated in this paper. As indicated in Tab. III, pilot control behavior will be compared for the aircraft pitch dynamics (2) and the double integrator dynamics (3) depicted in Fig. 3. For direct comparison with the results described by McRuer et al. and extrapolation of the results to multimodal piloting tasks, the control task is also performed both with and without additional physical pitch motion feedback.

TABLE III
EXPERIMENTAL CONDITIONS.

	no motion	motion
aircraft dynamics, (2)	C1	C2
double integrator dynamics, (3)	C3	C4

Five subjects performed the four experimental conditions listed in Tab. III. All participants were students or staff of the Faculty of Aerospace Engineering. Two subjects were pilots and all had experience with similar manual control tasks from previous human-in-the-loop experiments.

Participants were instructed to minimize the pitch tracking error, i.e., the signal that was presented on the visual display. Five repetitions of each experimental condition per subject were collected as the measurement data. Before performing the measurement runs, all subjects performed a considerable number of training runs, until their proficiency in performing the tracking task had clearly reached an asymptote. After each run subjects were informed of their tracking score – defined as the rms of the error signal e – in order to motivate them to constantly control at their maximum level of performance.

D. Pilot Model Identification

The parameters of the multi-channel pilot model depicted in Fig. 2 were estimated using a time-domain maximum likelihood estimation (MLE) procedure [3] for all experimental conditions listed in Tab. III. Note that for conditions C1 and C3, where no motion cues were available to the participants, only the model for the pilot visual response, $H_{pv}(j\omega)$, was fitted to the data. For every condition of every subject, the averaged data of five measurement runs were used as input to the estimation algorithm. Averaging the time-domain data

reduces the remnant power in the signals, thereby increasing the accuracy of the parameter estimation results.

As the results in the original work of McRuer et al. [7], [8] were based on experiments without physical motion cues, the main comparison of required pilot model equalization structures will be performed using the experimental conditions without physical motion (C1 and C3). For every data set for these no-motion conditions, four different pilot models were fitted, corresponding to the pilot equalization structures listed in Tab. I. For an evaluation of the effects of additional motion cues on control behavior, the full pilot model was estimated for conditions C2 and C4 with only the equalization forms found to be most suitable for both types of controlled dynamics.

IV. RESULTS

A. Pilot Model Equalization Comparison

Fig. 7 gives the mean estimated pilot visual response functions for the aircraft dynamics without physical motion cues. Although a pilot model with the 4 different equalization settings A-D was fitted, only equalizations A-C are given in the figure as the responses of C and D are highly similar. With the Fourier coefficients method (FC), the pilot describing function and the standard deviation thereof can be calculated analytically [12]. These are provided in Fig. 7 for reference.

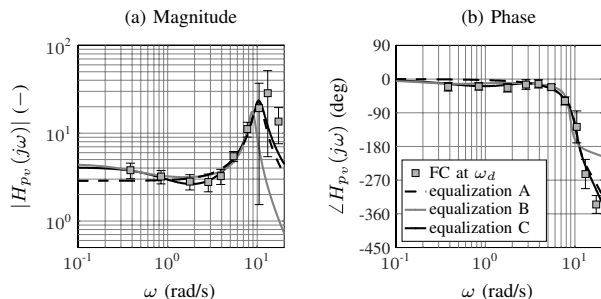


Fig. 7. Mean pilot model estimated frequency responses with different equalization settings for aircraft pitch dynamics (five subjects, condition C1).

As can be observed in Fig. 7, the pilot model with equalization C gives the most accurate results in the frequency domain, as it completely coincides with the results from the Fourier coefficients method. The equalization proposed by McRuer [9] for aircraft dynamics (B, see Tab. I) provides an acceptable fit at low frequencies, as it is able to capture the pilot lag equalization in that frequency range. At higher frequencies, however, equalization B shows large deviations from the Fourier coefficients, as this equalization form does not allow for generating high-frequency lead in addition to the lag. The pilot equalization with only a lead term (A) is able to capture the high-frequency magnitude response (Fig. 7(a)) with reasonable accuracy. A significant deviation can, however, be observed in the phase response around 1 rad/s (Fig. 7(b)). This clearly demonstrates the need for a lag term in the equalization dynamics.

The accuracy of the multimodal pilot model in the time domain can be evaluated using the variance accounted for

(VAF) [10]. The VAF indicates the amount of variance in the measured pilot control signal that can be described by the linear model fit. The mean VAF for the two different controlled dynamics and the four pilot equalizations is given in Fig. 8.

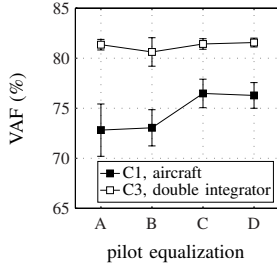


Fig. 8. Mean pilot model variance accounted for (VAF) for different equalization settings (five subjects, conditions C1 and C3).

For the aircraft dynamics, the figure clearly shows the need for the double lead term in the pilot equalization, as the achieved VAF is markedly higher for equalization C and D. Fig. 8 indicates that equalization B performs better than A in describing the pilot output in the time domain. This result confirms the frequency-domain results from Fig. 7. From Fig. 8 it can be concluded that equalization structures A and C are the most appropriate for describing pilot control behavior measured for conditions C1 and C3, respectively.

Fig. 9 gives the open-loop frequency response functions for control of aircraft and double integrator dynamics for the no motion conditions (C1 and C3). The open-loop frequency response functions are calculated with the pilot visual response, estimated with MLE, using the following relation: $H_{ol}(j\omega) = H_{p_v}(j\omega)K_{\delta_e, u}H_{\theta, \delta_e}(j\omega)$. The estimates are calculated from the pilot model with equalization A and C for double integrator and aircraft dynamics, respectively. Again, Fourier coefficients were used to calculate estimates of the open-loop describing functions for reference. The Fourier coefficients indicate that the MLE estimates provide a high accuracy in the frequency domain. In addition to the open-loop responses, the frequency responses of the controlled dynamics are depicted in gray.

Fig. 9 indicates that, for both controlled dynamics, the open-loop frequency responses are a single integrator [7] for frequencies around the crossover frequency ω_c (indicated with the slanted solid lines). The crossover frequencies are around 3 rad/s for both controlled dynamics, but found to be slightly higher for the aircraft dynamics. Similar values for the crossover frequency for double integrator dynamics were also found by McRuer and Jex [8]. Note from Fig. 9(a) that the short period dynamics of the aircraft around 2.76 rad/s still clearly affect the open-loop response for condition C1.

B. The Effect of Motion Cues

Fig. 10 gives the mean pilot frequency response functions for the four conditions listed in Tab. III. The average pilot model parameters for these responses are given in Tab. IV. Fig. 10 and Tab. IV clearly indicate the higher visual gain at

For the double integrator dynamics (C3), the different equalization settings perform equally well with an average VAF of around 82%. Note the slight reduction in VAF and increase in variance for equalization B, which is caused by the presence of a superfluous lag term. For equalizations C and D, the extra lead contributions can cancel out the effects of the lag, yielding fits similar to those obtained for A.

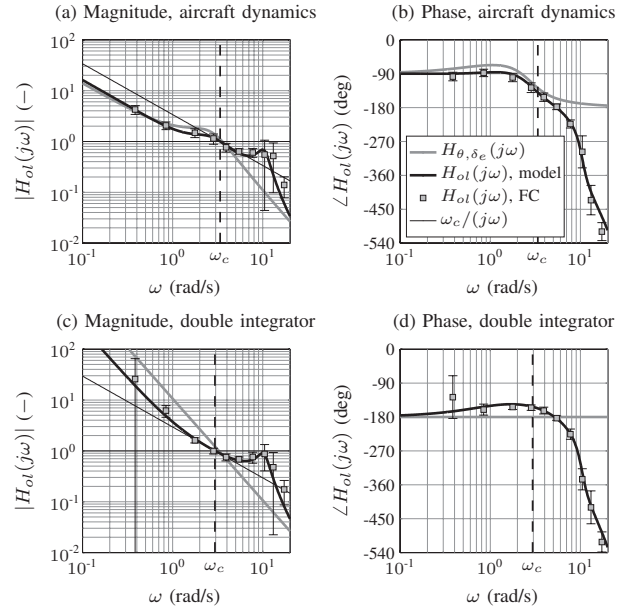


Fig. 9. Average open-loop responses for control of aircraft dynamics and double integrator dynamics (five subjects, conditions C1 and C3, respectively).

lower frequencies adopted for control of the aircraft dynamics. This is a result of the much lower gain of the aircraft dynamics at lower frequencies compared to double integrator dynamics (see Fig. 3). In addition, note the remarkable equivalence of the pilot vestibular responses for both sets of dynamics.

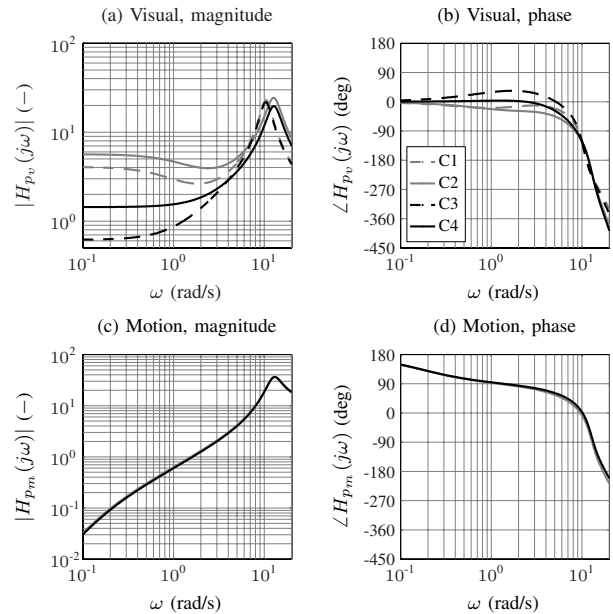


Fig. 10. Comparison of average pilot responses to visual and motion cues for control of aircraft and double integrator dynamics (five subjects).

An increased visual gain K_v is found for both types of controlled dynamics when physical motion cues are present. The

TABLE IV
AVERAGE PILOT MODEL PARAMETERS FOR EACH CONDITION.

Cond.	K_v (-)	T_L (s)	T_I (s)	K_m (-)	τ_v (s)	τ_m (s)	ω_{nm} (rad/s)	ζ_{nm} (-)
C1	4.07	0.44	1.32	-	0.21	-	10.50	0.14
C2	5.65	0.32	0.90	3.79	0.26	0.19	12.74	0.18
C3	0.62	0.98	-	-	0.23	-	10.41	0.14
C4	1.44	0.38	-	3.55	0.28	0.17	12.78	0.18

results further indicate (see Tab. IV) that for both controlled dynamics the visual lead constant T_L decreases as physical motion is available. Note the similar effect of motion on the lag time constant T_I for the pilot model for aircraft dynamics, hinting at a coupling between pilot lead and lag equalizations. The decrease in visual lead is compensated for by the additional pilot lead generated from the vestibular response $H_{p_m}(j\omega)$, see Fig. 10. The human vestibular system provides a much more efficient way of providing lead information [11], due to the smaller vestibular time delay. The visual perception delay τ_v increases for both dynamics if motion cues are available. The parameters of the neuromuscular system model are found to be strikingly equal for both controlled dynamics, both with and without physical motion cues. A significant increase in neuromuscular frequency ω_{nm} is observed when motion cues are available. These effects of motion cues on the pilot model parameters are consistent with previous research [2], [11].

V. DISCUSSION

The study described in this paper emphasizes the value of the model introduced by McRuer et al. [7], [8] for describing pilot control behavior during compensatory tracking. Pilot model estimation results clearly indicate that the pilot equalization term included in this model suffices for describing pilot equalization during control of double integrator dynamics, which then takes the form of a pure lead.

For the linearized aircraft pitch dynamics considered in this study, the equalization dynamics included in the model described in [7] are not found to suffice, due to the fact that pilots generated both mid-frequency lag and high-frequency lead. Addition of a second lead term to the pilot equalization transfer function is found to provide the means for modeling both these phenomena. A pilot equalization with a single lag and a squared lead term (C) is seen to perform best in representing the time- and frequency-domain pilot responses. Even though the time constants corresponding to both lead terms do not necessarily have to be equal, no improvement in fit is observed for an equalization with two independent lead terms (D). The extra parameter, however, leaves the optimization problem overdetermined.

The effect of physical motion feedback on pilot equalization was investigated by providing additional pitch rotational motion cues during both experiments. For both types of dynamics, measured pilot responses clearly indicate that pilots select the same equalization form for tasks with and without motion cues. Changes in the values of equalization parameters, however, indicate pilots do optimize their control strategy to

the availability of physical motion information. Such results of motion feedback are typical for tasks where direct motion cues (no washout) are provided in the controlled degree of freedom.

VI. CONCLUSIONS

A set of experiments was performed in the SRS to investigate pilot equalization for control of aircraft dynamics, as opposed to double integrator dynamics. It is found that a pilot equalization with a squared lead and a single lag term provides significantly better results compared to the single lead and lag equalization proposed in literature. For both types of dynamics, the presence of physical motion cues was not found to cause pilots to adapt the structure of their equalization dynamics. An increased visual perception gain and visual time delay, and a decrease in the visual lead time constant, however, do reveal pilots' optimization of the adopted operating point for their selected equalization form.

ACKNOWLEDGMENTS

This research was supported by the Technology Foundation STW, the applied science division of NWO, and the technology program of the Ministry of Economic Affairs.

REFERENCES

- [1] M. Steurs, M. Mulder, and M. M. van Paassen, "A cybernetic approach to assess flight simulator fidelity," in *Proceedings of the AIAA Modeling and Simulation Technologies Conference and Exhibit, Providence, Rhode Island, 16-19 August 2004*, 2004, AIAA-2004-5442.
- [2] P. M. T. Zaal, D. M. Pool, J. de Bruin, M. Mulder, and M. M. van Paassen, "Use of pitch and heave motion cues in a pitch control task," *Journal of Guidance, Control and Dynamics*, vol. 32, no. 2, pp. 366-377, March-April 2009.
- [3] P. M. T. Zaal, D. M. Pool, Q. P. Chu, M. M. van Paassen, M. Mulder, and J. A. Mulder, "Modeling human multimodal perception and control using genetic maximum likelihood estimation," *Journal of Guidance, Control and Dynamics*, unpublished.
- [4] T. J. Groot, H. J. Damveld, M. Mulder, and M. M. van Paassen, "Effects of aeroelasticity on the pilot's psychomotor behavior," in *Proceedings of the AIAA Atmospheric Flight Mechanics Conference and Exhibit, 21-24 August 2006, Keystone, Colorado*, 2006, AIAA-2006-6494.
- [5] H. J. Damveld, "A Cybernetic Approach to Assess the Longitudinal Handling Qualities of Aeroelastic Aircraft," Ph.D. dissertation, Delft University of Technology, Faculty of Aerospace Engineering, May 2009.
- [6] J. I. Elkind, "Characteristics of Simple Manual Control Systems," Ph.D. dissertation, Massachusetts Institute of Technology, June 1956.
- [7] D. T. McRuer, D. Graham, E. S. Krendel, and W. Reisener Jr., "Human Pilot Dynamics in Compensatory Systems. Theory, Models and Experiments with Controlled Element and Forcing Function Variations," Air Force Flight Dynamics Laboratory, Wright-Patterson AFB (OH), AFFDL-TR 65-15, August 1965.
- [8] D. T. McRuer and H. R. Jex, "A review of quasi-linear pilot models," *IEEE Transactions on Human Factors in Electronics*, vol. HFE-8, no. 3, pp. 231-249, 1967.
- [9] D. T. McRuer, "Pilot modeling," in *AGARD-LS-157*. North Atlantic Treaty Organisation, Advisory Group for Aerospace Research and Development, 1988, pp. 2-1 - 2-30.
- [10] F. M. Nieuwenhuizen, P. M. T. Zaal, M. Mulder, M. M. van Paassen, and J. A. Mulder, "Modeling human multi-channel motion perception and control using linear time-invariant models," *Journal of Guidance, Control, and Dynamics*, vol. 31, no. 4, pp. 999-1013, 2008.
- [11] R. J. A. W. Hosman, "Pilot's Perception and Control of Aircraft Motions," Ph.D. dissertation, Delft University of Technology, Faculty of Aerospace Engineering, 1996.
- [12] M. M. van Paassen and M. Mulder, "Identification of human operator control behaviour in multiple-loop tracking tasks," in *Proceedings of the Seventh IFAC/IFIP/IFORS/IEA Symposium on Analysis, Design and Evaluation of Man-Machine Systems, Kyoto, Japan*. Pergamon, 1998, pp. 515-520.